Sol-gel synthesis of barium hexaferrite and their catalytic application in methyl ester synthesis

IOP Conf. Series: Materials Science and Engineering **509** (2019) 012103 doi:10.1088/1757-899X/509/1/012103

Sol-gel synthesis of barium hexaferrite and their catalytic application in methyl ester synthesis

Nur Izzana Sulaiman[1], Mohamad Abu Bakar[1,*], Noor Hana Hanif Abu Bakar[1], Mohd Hazwan Hussin[2]

[1] Nanoscience Research Laboratory, School of Chemical Sciences, Universiti Sains Malaysia, 11800 Minden, Penang, Malaysia
[2] Materials Technology Research Group (MaTReC), School of Chemical Sciences, Universiti Sains Malaysia, 11800 Minden, Penang, Malaysia
* Corresponding author: bmohamad@usm.my

Abstract. Fine barium hexaferrite, $BaFe_{12}O_{19}$ has been synthesized through sol-gel technique using barium chloride dihydrate ($BaCl_2.2H_2O$) and iron (III) chloride hexahydrate ($FeCl_3.6H_2O$) as starting materials. The $BaFe_{12}O_{19}$ particles were characterized by X-ray diffraction (XRD), TGA, Fourier-Transform Infrared Spectroscopy (FTIR) and N_2 Adsorption-Desorption Isotherm. XRD revealed that high calcination temperature is beneficial for the formation of fine $BaFe_{12}O_{19}$. The results show that the crystallite size of the produced samples increased with an increase in calcination temperature. It was found that the crystalline $BaFe_{12}O_{19}$ phase was well formed above 700°C. $BaFe_{12}O_{19}$ was as employed as a new heterogeneous acid catalyst for the application production of methyl ester. The suitability of $BaFe_{12}O_{19}$ as catalyst for esterification of palmitic acid was evaluated on the basis of catalyst dosage, reaction time and molar ratio of the reactants to optimize the reaction condition. The catalyst gave excellent methyl ester yield of 91.7% at optimum conditions. The optimum esterification conditions for of 0.5 g palmitic acid are; 2 wt.% of $BaFe_{12}O_{19}$ with 1:15 molar ratio of palmitic acid to methanol at reaction temperature 120°C for 2 hours.
Keywords: barium hexaferrite; sol-gel; esterification; catalyst; methyl ester

1. Introduction

Energy has become an important human issue since the beginning of 18th century. The most important global energy production comes from fossil fuel. This source of energy is non-renewable. In order to meet future demands, alternative ways of producing fuel must be taken. Biodiesel is an environmentally friendly fuel which is commonly produced through the esterification of fatty acids with low molecular weight alcohols in the presence of homogenous basic catalysts such as sodium and potassium hydroxides [1]. Esterification is the reaction that takes place in chemical industries where efficient acid catalyst is required to obtain good yields of methyl ester at better selectivity [2]. Homogenous catalysts such as H_2SO_4, HF, H_3PO_4 are usually utilized in esterification reactions. However, there are several disadvantages when using these catalysts. The catalysts often cause serious issues in product separation, catalyst reuse and disposal [3]. Thus, to manage these problems, mineral acids can be replaced by solid acids such as metal oxides, zeolites and also clays. The use of solid acids have been a major research area as it is an environmentally benign processes which use less hazardous chemicals [4]. This process is quite simple with negligible environment problems. Thus, the development of low cost solid catalysts which are easily reusable has become popular in recent research efforts [5].

Ordinary heterogeneous catalysts such as single metal oxides, zeolites and supported alkali-metal/metal ion have been seen to be efficient for the production of biodiesel. In recent years, heterogeneous catalyst for methyl ester synthesis have focused on metal oxides. These catalysts are low in production costs compared to their homogenous counterparts [6, 7]. Several factors such as surface area, pore size, pore volume and active site concentration are important factors in increasing the catalyst efficiency. Previous studies showed that tin oxide shows good catalytic activity for soybean oil methanolysis. The reaction achieved up to 90% in 3 hours at 60°C [8]. Besides, zirconium oxide, titanium oxide and zinc oxide are among other metal oxides that have been reported for biodiesel production due to their acidic properties [9]. Nevertheless, single metal oxides have some disadvantages such as these catalysts are show poor strength and possessed low resistance to atmospheric CO_2. They also have generally lower catalytic performance [10]. To improve the method, the utilization of binary or tertiary (solid mixed) metal oxide catalysts for the production of biodiesel has gained attention in recent years.

Solid mixed metal oxide generally refers to material consisting of two or more metal oxides. The advantages of mixed metal oxides are their low corrosiveness and also ease of regeneration and reuse. $BaFe_{12}O_{19}$ is a hard magnetic material with high coercitivity and also large saturation magnetization [11]. Aside from being permanent magnet, $BaFe_{12}O_{19}$ has been used to increase the capacity in information storage [12, 13]. $BaFe_{12}O_{19}$ is a new heterogeneous catalyst in esterification study so far. The study on barium-based binary and tertiary oxides in esterification study is rarely reported. Previous studies were conducted by Sherstyuk *et al.* [14, 15]. They successfully prepared Ba-Al-O (viz. $BaAl_{13.2}O_{20.8}$ and $BaAl_{12}O_{19}$) and Ba-La-O (viz. $BaLa_2O_4/La_2O_3$ and $Ba_{0.04}La_{1.96}O_3$) in binary system. This studies were used precipitation and calcination method to investigate their application in the transesterification of rapeseed oil. This binary system achieved ~100% at the optimum condition for conversion of rapeseed oil over Ba-Al-O and the result showed the stability of Ba-Al-O is higher than Ba-La-O binary catalysts. In this work, we synthesized $BaFe_{12}O_{19}$ for esterification of palmitic acid with methanol to methyl palmitate as in (1) [16]. Catalyst dosage, reaction time and molar ratio of the reactants were varied to optimize the reaction conditions. The catalytic performance is reported in this study.

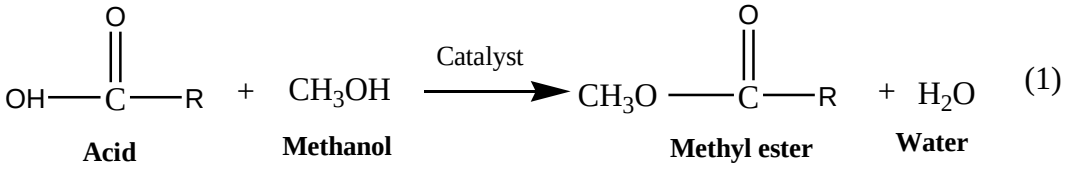

2. Experimental

2.1. Materials

Palmitic acid was obtained from Fluka, $FeCl_3.6H_2O$ was supplied by Sigma-Aldrich whereas $BaCl_2.2H_2O$ by BDH Laboratory Supplies. Glycine was purchased from BioLab Medical Unit. Methanol, 2-propanol and cyclohexane of QREC brand was supplied by Brightchem Sdn Bhd. The chromatographic methyl ester standard, methyl palmitate was supplied by Fluka. All the chemicals were of analytically pure grade.

2.2. Preparation of the Catalyst

The starting materials used for this study were $BaCl_2.2H_2O$ and $FeCl_3.6H_2O$ powders. The synthesis of the $BaFe_{12}O_{19}$ was by sol-gel technique followed by calcination. Typically, 1.29 g of $BaCl_2.2H_2O$ was dissolved in 40 mL distilled water heated in an oil bath at 50°C for several minutes. Then, $FeCl_3.6H_2O$ was added. The mixture was stirred for 2 hours under reflux. Proper amount of glycine was added in the mixture. The product which is in gel form was separated via rotary evaporator and washed with distilled

water. The catalyst was then dried overnight in the vacuum oven and followed by calcination at 600-900°C for an hour.

2.3. Characterization of the Catalyst

The structure and phase of the samples were characterized by powder XRD technique in the 2θ range of 30-80°. The reflection of the peaks obtained from this characterization were compared with the JCPDS-PDF database. Functional group analysis of the samples was done on Perkin-Elmer System 2000 using KBr pellet where the spectra were recorded in the range of 4000-500 cm^{-1}. The surface area of the sample was determined using Brunauer-Emmett-Teller (BET) method and the surface was analysed via N_2 adsorption-desorption isotherm. The thermal analysis was done in order to understand the thermostability of the samples using TGA 7 (Perkin-Elmer) at a heating rate of 20°C min^{-1} from 30 to 900°C and held for 5 minutes at 900°C.

2.4. Methyl Palmitate Production

Production of the methyl palmitate was performed in an autoclave at the temperature of 120°C for 2 hours. The ingredients of the reaction mixture were completely removed by distillation under pressure. The residual methyl palmitate was subjected to GC chromatography. The GC was carried out on a Hitachi 263-30 instrument equipped with a flame ionization detector. Instrument setting: Injector temperature = 200°C and detector temperature = 250°C. The percentage of methyl palmitate yield was calculated based on equation (2) below.

$$\text{Methyl Ester Yield} = \frac{\text{Total ME area from GC x Weight of product}}{\text{Weight of acid}} X\ 100\% \quad (2)$$

3. Result and Discussion

3.1. Characterization of the Catalyst

3.1.1. XRD. In this study, sol-gel technique was used for the synthesis of $BaFe_{12}O_{19}$. The catalyst was prepared at different calcination temperature. Calcination temperature plays an important role in the formation of $BaFe_{12}O_{19}$ phase. The purpose of the characterization of catalyst by XRD is to determine changes in the structure, phase and also crystallinity of $BaFe_{12}O_{19}$ with different calcination temperature (600-900°C). The XRD patterns are presented in Fig. 1. The diffractogram patterns show major peaks at 2θ values of 33.1°, 35.7° and 54.1°. These peaks are indexed to the (112), (114) and (217) planes of $BaFe_{12}O_{19}$ with a hexagonal crystal structure that confirm with database JCPDS card No. 78-0133 [17, 18].

Based on the results in Fig. 1, at a temperature below 600°C, there are some intermediate phases identified such as γ-Fe_2O_3 and $BaFe_2O_4$. Crystalline single $BaFe_{12}O_{19}$ phase was formed at and above 700°C. For the sample calcined at 700°C and above, $BaFe_{12}O_{19}$ became the major phase while $BaFe_2O_4$ and γ-Fe_2O_3 existed as a minor phase. $BaFe_2O_4$ was diminished at a calcination temperature of 700°C and above. The result of XRD shows that $BaFe_{12}O_{19}$ structure was detected without any other impurities for powders calcined at 700°C, 800°C and 900°C. It means that all intermediate phases were transformed into $BaFe_{12}O_{19}$ phase when the calcination temperature is above 700°C. Table 1 presented the crystallite size of the samples which was calculated using Scherrer's formula. The crystallite size increased with the increase in calcination temperature as the crystal growth increases rapidly which can be assign by more agglomerated crystals [19]. The result appears that a higher calcination temperature enhances atomic mobility and causes grain growth which is resulting in better crystallinity [20].

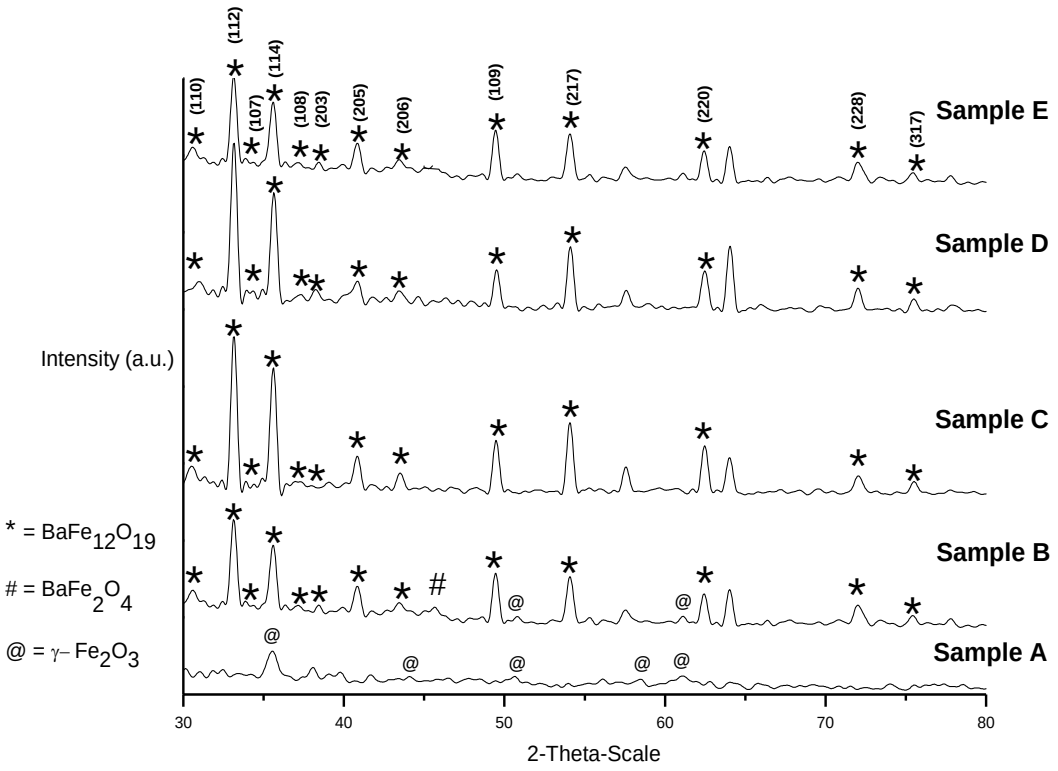

Figure 1. XRD pattern of the $BaFe_{12}O_{19}$ samples calcined at various temperatures; Sample A (Uncalcined), B (600°C), C (700°C), D (800°C), E (900°C).

Table 1. Crystallite size, Specified surface area and total pore volume of the $BaFe_{12}O_{19}$ samples.

Samples	Temperature Treatment (°C)	Crystallite size (nm)	Specified surface area (m^2/g)	Total pore volume (cm^3/g)
A	Uncalcined	Amorphous	0.5426	0.00347
B	600	42.10	2.7823	0.00657
C	700	53.81	7.3917	0.02318
D	800	56.13	3.3843	0.01734
E	900	58.14	2.5093	0.00667

3.1.2. FTIR. Fig. 2 illustrates the FTIR spectra of the samples treated at different temperatures (600-900°C). As shown in Fig. 2, the adsorption bands at around 3400-3700 cm^{-1} are assigned to the O-H group for the stretching vibration of adsorbed water [21]. The adsorption band due to the bending mode of water molecules are observed at 1620-1630 cm^{-1} and can be due to the presence of water hydration in the samples [22]. The infrared spectra of $BaFe_{12}O_{19}$ obtained at different calcination temperatures exhibit vibration bands at 577, 574 and 587 cm^{-1} which corresponds to the vibrations of metal-oxygen stretching of $BaFe_{12}O_{19}$ [23, 24]. The result is in agreement with XRD results which suggests that single $BaFe_{12}O_{19}$ powders can be obtained when calcined at and above 700°C. The increasing calcination temperature improved the $BaFe_{12}O_{19}$ phase formation.

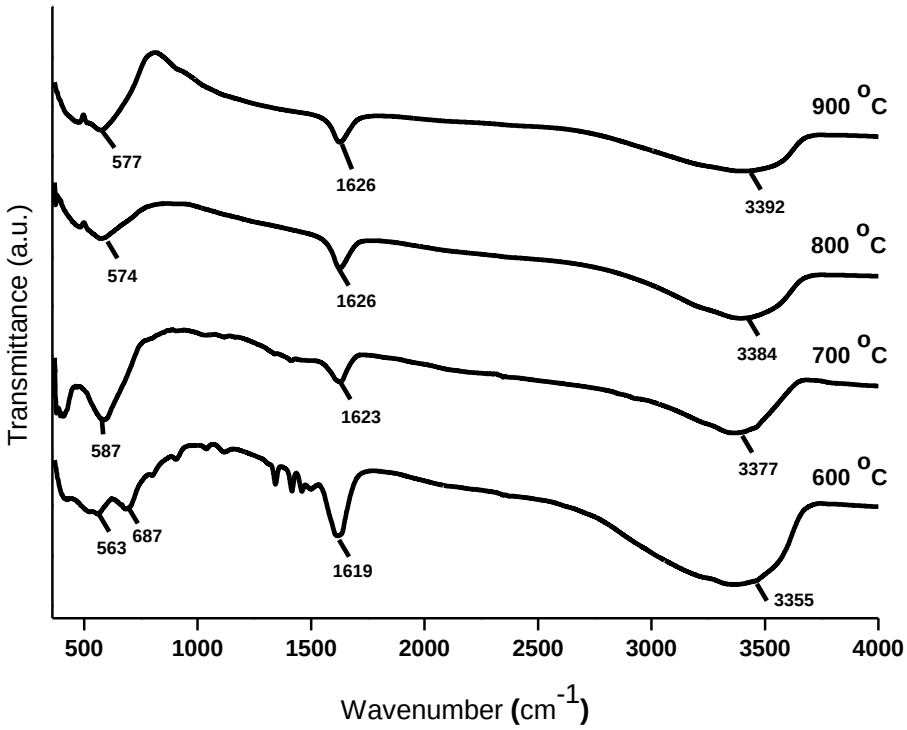

Figure 2. FTIR spectra of the $BaFe_{12}O_{19}$ samples calcined at various temperatures (600°C-900°C).

3.1.3. Thermal Analysis. The TG curve shown in Fig. 3 was obtained to investigate the thermal stability of materials at calcination temperature of 700°C. The first weight loss of 6.5% was due to the removal of physisorbed water in the temperature range of up to 158°C. The second weight loss is because of the removal of chemisorbed water and decomposition of the hydroxide. This second weight loss was around 2.1% which occurs at 158-196°C and the subsequent weight loss at around 196-284°C are due to further decomposition of the samples. At 264-480°C and 480-635°C, additional weight reduction occurred due to the crystallization of $BaFe_{12}O_{19}$ [25]. There is no weight loss above 635°C which confirms the high thermal stability of the catalyst synthesized by sol-gel method [26].

3.1.4. N_2 Adsorption-Desorption Isotherm

The surface properties of $BaFe_{12}O_{19}$ prepared at various calcination temperatures were analysed via N_2 adsorption-desorption isotherms. The results are shown in Fig. 4. The isotherm of $BaFe_{12}O_{19}$ samples were classified as type I and IV behaviour based on the IUPAC classification scheme [27]. All samples show sharp increase at relatively high pressure. This indicates the presence of mesopores. Type IV isotherm indicated that the samples were given by many mesoporous adsorbents due to high pressure behaviour. The adsorption of nitrogen molecules occurred between the relative pressure P/Po of zero to < 0.3. The steep at the initial region shows that strong adsorption occurred. This strong gas-solid interaction may influence the interaction between the catalyst and reactants. This is important for catalysts as the adsorption mostly occurred on the external surface. At P/Po = 0 to P/Po = 0.9, the samples started to interact in the pore [28]. Then, at P/Po < 1.0 which was at higher pressure, the isothermal curve increasingly shapes. The samples demonstrated a limiting uptake which is controlled by the accessible micropore volume. Based on IUPAC classification, all samples present a H3-type hysteresis loop which showed the capillary condensation of mesopores.

Meanwhile, increasing the calcination temperature from uncalcined to 700°C influenced the BET surface area which increased from 0.5426 m^2/g to 7.3917 m^2/g. From Table 1, the largest specific surface area was obtained for the sample calcined at 700°C. A similar trend was observed for the total pore volume result. It was found that further increase in the temperature exceeding 700°C resulted in a

decrease in the surface area to 3.3843 m^2/g and 2.5093 m^2/g for samples calcined at 800°C to 900°C respectively. By increasing of calcination temperature further, the pore volume decreases which indicates the changes of the crystal wall structure as confirmed by XRD measurements [29].

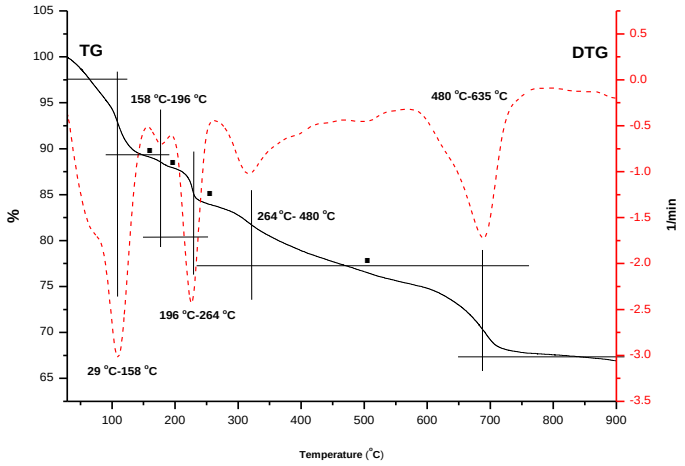

Figure 3. Typical TGAand DTG curve of the $BaFe_{12}O_{19}$.

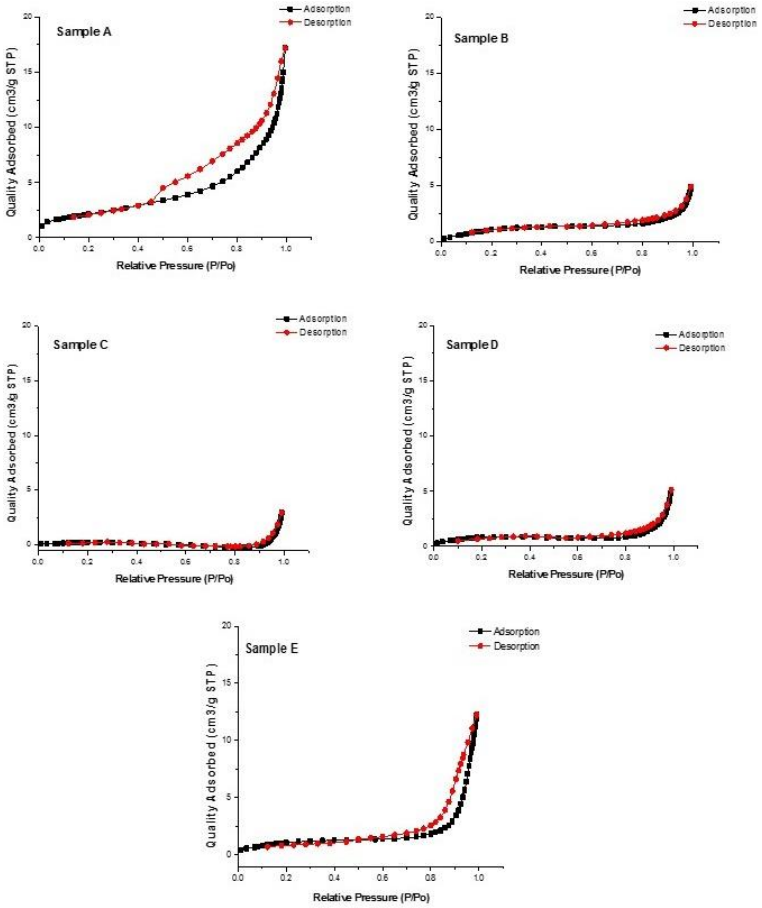

Figure 4. N_2-adsorption desorption isotherm plot at the calcination temperature: Sample A (Uncalcined), B (600°C), C (700°C), D (800°C), E (900°C).

3.2. Catalytic esterification of palmitic acid with methanol

3.2.1. Effect of Calcination Temperature. The effect of calcination temperature on the activity of $BaFe_{12}O_{19}$ calcined at 600-900°C using molar ratio of palmitic acid/methanol 1:15 and 2 wt% of catalyst dosage and the results are presented in Fig. 5(A). Based on the result, it can be seen that calcination at 700°C exhibits the highest activity. At 2 hours' reaction, the percentage of methyl ester yield obtained was 91.7%. It can be related to the highest pore volume as indicated in Table 1. Pore diffusion becomes an important factor rather than surface area due to methyl ester molecules which are large and consists of long alkyl chains. Calcining $BaFe_{12}O_{19}$ at low temperatures (600°C) and very high temperatures (800-900°C) will decrease the catalytic activity of the catalyst. This is because at low temperature which is 600°C, the crystallinity of $BaFe_{12}O_{19}$ is not created well. In contrast, at 800-900°C, the catalyst loses its porosity [30]. The catalyst synthesized at 700°C in the present study showed a good catalytic activity with the highest percentage of methyl ester yield.

3.2.2. Influence of catalyst dosage. Fig. 5 (B) shows the effect of catalyst dosage on the percentage of methyl ester yield. The catalysts chosen was $BaFe_{12}O_{19}$ calcined at 700°C as it exhibits the highest activity. As the amount of the catalyst dosage increased from 0 to 3 wt% of $BaFe_{12}O_{19}$, the percentage of methyl ester yield also increased from less than 5% in the absence of catalyst to 91.7%. The optimum amount of catalyst dosage was 2 wt% because the percentage of methyl ester yield remained almost constant above this dosage. The barium ion that holds the ferrite structure together is postulated to act as a Lewis acid site for connection of fatty acids for formation of methyl esters. Based on the result, it is important to clarify that the esterification reaction can occur in the absence of the catalyst. However, the percentage of methyl ester yield was less than 5%.

3.2.3. Effect of reaction time. The effect of reaction time on the percentage of methyl ester yield was studied. Results are shown in Fig. 5 (C). The percentage of methyl ester yield levelled off as the products reached a near-equilibrium composition after 2 hours. The result shows that as the reaction progresses above 2 hours, the reaction reached a plateau due to no significant differences in the yield of methyl ester. This result demonstrated that the catalyst had a very high reactivity to catalyse esterification reaction. In conclusion, the optimum reaction time for the reaction was 2 hours.

3.2.4. Influence of palmitic acid: methanol molar ratio. The esterification reaction was investigated by mixing palmitic acid with methanol in the ratio 1:8 to 1:20 with 2 wt% of $BaFe_{12}O_{19}$ in an autoclave to study the effect of molar ratio on the catalytic activity. Then, the autoclave was heated in a furnace at 120°C for 2 hours. Based on the result, increasing the volume of methanol increased the percentage of methyl ester yield within the same reaction time. Based on Fig. 5 (D), the percentage of methyl ester yield increased from 59.2% to 91.7% when the molar ratio 1:8 to 1:15. The highest percentage (91.7%) was achieved at molar ratio 1:15 of palmitic acid: methanol. The reaction was continued at molar ratio 1:20 and it can be seen that the percentage of methyl ester yield decreased slightly. The result probably infers that dilution effect may have taken place [31].

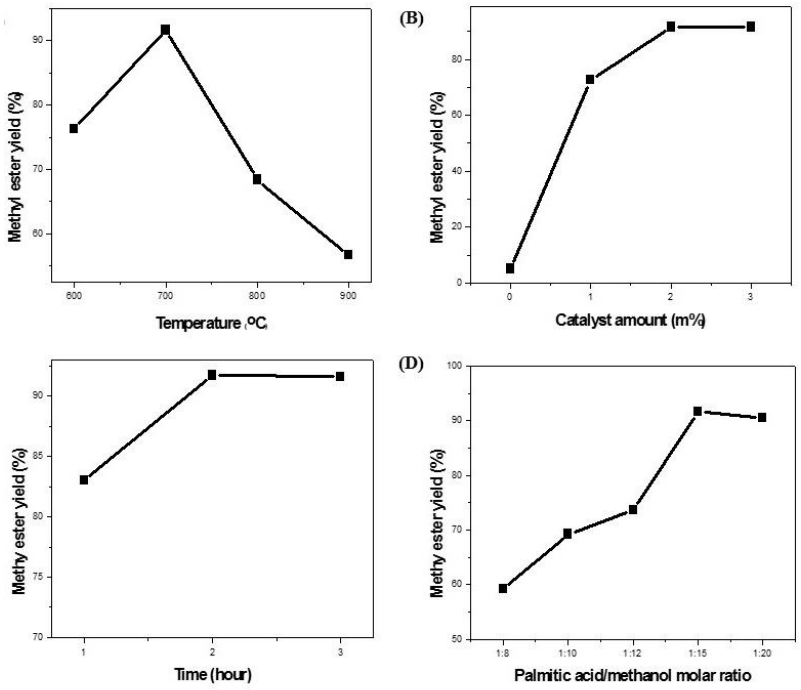

Figure 5. Graphs of methyl ester yield (%) against **(A)** calcination temperature, **(B)** catalyst amount (wt%), **(C)** reaction time (hours) and **(D)** molar ratio of palmitic acid/methanol.

4. Conclusion

$BaFe_{12}O_{19}$ catalysts were successfully prepared at different calcination temperatures via the sol-gel method. The catalysts were characterized and proven as a heterogeneous catalyst for the esterification reaction of palmatic acid with methanol. XRD patterns revealed that at low temperature, the samples were amorphous with some intermediate phase. However, at high calcination temperatures, $BaFe_{12}O_{19}$ exhibited crystalline structures. The specified surface area increased as the calcination temperature of samples increased towards 700°C. It also corresponds to the total pore volume of the samples. Maximum catalytic activity for the esterification reaction was achieved at the molar ratio of palmatic acid/methanol 1:15 with the reaction temperature 120°C for 2 hours in the presence of 2 wt% catalyst affording a methyl ester yield of 91.7%. The influence of all the parameters will affect the percentage of methyl ester yield. The $BaFe_{12}O_{19}$ catalyst showed good catalytic activity performance in the esterification reaction.

Acknowledgements

The authors would like to acknowledge the financial support from Research University Grant Scheme (RUI) 1001/PKIMIA/811311 Universiti Sains Malaysia (USM).

References

[1] Marchetti J M, Miguel V and Errazu A 2007 Possible methods for biodiesel production *Renew. Sust. Energy Rev.* **11** 6 1300-11
[2] Nagaraju N and Shamshuddin S 2005 Solid acids in liquid phase esterification *Indian Journal of Chemistry-A* **44A** 1165-70
[3] Peter O, Chidi O and Iheanacho M 2012 The preparation and application of environmentally benign titanium pillared clay catalyst for esterification of ethanol and acetic acid *Am. Chem.*

Sci. J. **2** 45-59
[4] Qiuyun Z, Hu L, Wenting Q, Xiaofang L, Yuping Z, Wei X and Song Y 2013 Solid acid used as highly efficient catalyst for esterification of free fatty acids with alcohols *China Pet. Process. Petrochemical Technol.* **15** 1 19-24
[5] Boey P-L, Ganesan S, Maniam G P, Khairuddean M and Lee S-E 2012 A new heterogeneous acid catalyst system for esterification of free fatty acids into methyl esters *Appl. Catal. A Gen.* **433** 12-7
[6] Helwani Z, Othman M, Aziz N, Fernando W and Kim J 2009 Technologies for production of biodiesel focusing on green catalytic techniques: a review *Fuel Process. Technol.* **90** 12 1502-14
[7] Borges M E and Díaz L 2012 Recent developments on heterogeneous catalysts for biodiesel production by oil esterification and transesterification reactions: a review *Renew. Sust. Energy Rev.* **16** 5 2839-49
[8] Macedo C, Abreu F R, Tavares A P, Alves M B, Zara L F, Rubim J C and Suarez P A 2006 New heterogeneous metal-oxides based catalyst for vegetable oil trans-esterification *J. Braz. Chem. Soc.* **17** 7 1291-6
[9] Zabeti M, Daud W M A W and Aroua M K 2009 Activity of solid catalysts for biodiesel production: a review *Fuel Process. Technol.* **90** 6 770-7
[10] Lee D-W, Park Y-M and Lee K-Y 2009 Heterogeneous base catalysts for transesterification in biodiesel synthesis *Catal. Surv. Asia* **13** 2 63-77
[11] Vu H, Nguyen D, Fisher J G, Moon W-H, Bae S, Park H-G and Park B-G 2013 CuO-based sintering aids for low temperature sintering of BaFe12O19 ceramics *J. Asian Ceram. Soc.* **1** 2 170-7
[12] Fujiwara T 1985 Barium ferrite media for perpendicular recording *IEEE Trans. Magn.* **21** 5 1480-5
[13] Yamamori K, Suzuki T and Fujiwara T 1986 High density recording characteristics for Ba-ferrite flexible disks *IEEE Trans. Magn.* **22** 5 1188-90
[14] Sherstyuk O, Ivanova A, Lebedev M, Bukhtiyarova M, Matvienko L, Budneva A, Simonov A and Yakovlev V 2012 Transesterification of rapeseed oil under flow conditions catalyzed by basic solids: MAl (La) O (M= Sr, Ba), MMgO (M= Y, La) *Appl. Catal. A Gen.* **419** 73-83
[15] Ivanova A, Sherstyuk O, Bukhtiyarova M, Kukushkin R, Matvienko L, Plyasova L, Kaichev V, Simonov A and Yakovlev V 2012 Performance of Ba-containing catalysts in the transesterification reaction of rapeseed oil with methanol under flow conditions *Catal. Commun.* **18** 156-60
[16] Turapan S, Yotkamchornkun C and Nuithitikul K 2010 Esterification of free fatty acids in crude palm oil with sulfated zirconia: Effect of calcination temperature *J. World Acad. Sci. Eng. Technol.* **41** 520-4
[17] Xu P, Han X and Wang M 2007 Synthesis and magnetic properties of BaFe12O19 hexaferrite nanoparticles by a reverse microemulsion technique *J. Phys. Chem. C* **111** 16 5866-70
[18] Mosleh Z, Kameli P, Ranjbar M and Salamati H 2014 Effect of annealing temperature on structural and magnetic properties of BaFe12O19 hexaferrite nanoparticles *Ceram. Int.* **40** 5 7279-84
[19] Gaber A, Abdel-Rahim M, Abdel-Latief A and Abdel-Salam M N 2014 Influence of calcination temperature on the structure and porosity of nanocrystalline SnO2 synthesized by a conventional precipitation method *Int. J. Electrochem. Sci.* **9** 1 81-95
[20] Chang Y-S 2008 The effects of heat treatment on the crystallinity and luminescence properties of YInGe2O7 doped with Eu3+ ions *J. Electron. Mater.* **37** 7 1024-8
[21] Indrayanah S, Rosyidah A, Setyawati H and Murwani I 2018 Performance of Magnesium Hydroxide Fluorides as Heterogeneous Acid Catalyst for Biodiesel Production *Rasayan J. Chem.* **11** 1 312-20
[22] Yeşilbaş M, Holmboe M and Boily J-F 2017 Cohesive Vibrational and Structural Depiction of

Intercalated Water in Montmorillonite *ACS Earth Space Chem.* **2** 1 38-47
[23] Singhal S, Namgyal T, Singh J, Chandra K and Bansal S 2011 A comparative study on the magnetic properties of MFe12O19 and MAlFe11O19 (M= Sr, Ba and Pb) hexaferrites with different morphologies *Ceram. Int.* **37** 6 1833-7
[24] Rahimi M, Kameli P, Ranjbar M, Hajihashemi H and Salamati H 2013 The effect of zinc doping on the structural and magnetic properties of Ni1− xZnxFe2O4 *J. Mater. Sci.* **48** 7 2969-76
[25] Kim S-G, Wang W-N, Iwaki T, Yabuki A and Okuyama K 2007 Low-temperature crystallization of barium ferrite nanoparticles by a sodium citrate-aided synthetic process *J. Phys. Chem. C* **111** 28 10175-80
[26] Jotania R, Khomane R, Chauhan C, Menon S and Kulkarni B 2008 Synthesis and magnetic properties of barium–calcium hexaferrite particles prepared by sol–gel and microemulsion techniques *J. Magn. Magn. Mater.* **320** 6 1095-101
[27] Sing K 1982 Reporting physisorption data for gas/solid systems with special reference to the determination of surface area and porosity (Provisional) *pac* **54** 11 2201-18
[28] Yang Y, Shukla P, Wang S, Rudolph V, Chen X-M and Zhu Z 2013 Significant improvement of surface area and CO 2 adsorption of Cu–BTC via solvent exchange activation *RSC Adv.* **3** 38 17065-72
[29] Sun Z-X, Zheng T-T, Bo Q-B, Du M and Forsling W 2008 Effects of calcination temperature on the pore size and wall crystalline structure of mesoporous alumina *J. Colloid Interface Sci.* **319** 1 247-51
[30] Eloka-Eboka A C, Igbum O G and Inambao F L 2014 Optimization and effects of process variables on the production and properties of methyl ester biodiesel *J. Energy South Afr.* **25** 2 39-47
[31] Di Serio M, Cozzolino M, Giordano M, Tesser R, Patrono P and Santacesaria E 2007 From homogeneous to heterogeneous catalysts in biodiesel production *Ind. Eng. Chem. Res.* **46** 20 6379-84